

Precise temperature estimation in the Tibetan crust from seismic detection of the α - β quartz transition

J. Mechie* GeoForschungsZentrum Potsdam, Telegrafenberg, 14473 Potsdam, Germany

S.V. Sobolev GeoForschungsZentrum Potsdam, Telegrafenberg, 14473 Potsdam, Germany, and
Institute of Physics of the Earth, Moscow, Russia

L. Ratschbacher Institut für Geologie, Technische Universität Freiberg, 09599 Freiberg, Germany

A. Y. Babeyko

G. Bock†

} GeoForschungsZentrum Potsdam, Telegrafenberg, 14473 Potsdam, Germany

A.G. Jones* Geological Survey of Canada, Ottawa, Ontario, Canada, and Department of Earth Sciences, Syracuse University, Syracuse, New York 13244, USA

K.D. Nelson†

K.D. Solon*

} Department of Earth Sciences, Syracuse University, Syracuse, New York 13244, USA

L.D. Brown Department of Earth and Atmospheric Sciences, Cornell University, Ithaca, New York 14853, USA

W. Zhao Chinese Academy of Geological Sciences, 26 Baiwanzhuang Road, Beijing 100037, China

ABSTRACT

In the deep crust, temperature, which is among the key parameters controlling lithospheric dynamics, is inferred by extrapolation from the surface using several assumptions that may fail in regions of active tectonics and fluid migration. In the rare case that temperatures of 700 °C or higher are exceeded in the upper and middle continental crust composed of quartz-rich felsic rocks, the α - β quartz transition (ABQT) will occur, generating a measurable seismic signature and offering the possibility for precisely estimating temperature from the known ABQT phase diagram. Here it is shown that all expected seismic features of the ABQT are met by the boundary between the upper and middle crust below the INDEPTH III profile in central Tibet. This finding implies that a temperature of 700 °C is achieved at a depth of 18 km under the southern Qiangtang block, which agrees with the depth to the top of a high electrical conductivity anomaly, likely representing partially melted crust. To the south in the northern Lhasa block, the ABQT is at 32 km depth, corresponding to a temperature of 800 °C. It thus appears that this seismic boundary representing the ABQT is the result of recent geologic processes rather than being a lithologic boundary.

Keywords: Tibet, α - β quartz transition, seismic profiles, crustal structure.

α - β QUARTZ TRANSITION

The phase transition from α -quartz, one of the most common minerals in Earth's crust, into the higher-symmetry β -quartz was first discovered in 1889 by LeChatelier (1889) and has been studied extensively since. The transition occurs at 575 °C at atmospheric pressure, and the symmetry change is accompanied by changes in volume and thermoelastic properties (Carpenter et al., 1998). The transition temperature increases linearly with pressure by 0.25 K/MPa and does not depend on other minerals in the rock. At high temperatures (>600 °C), quartz is known to be mechanically weak and unable to maintain any significant deviatoric stress (Jaoul et al., 1984), and thus the pressure in quartz-rich rocks at these temperatures must be close to lithostatic, a known function of depth. This means that the temperature of the α - β quartz transition (ABQT) in quartz-rich rocks should depend only

on depth. Hence, if this transition were detected at some depth, then it is possible to know precisely the temperature at that depth from the phase-transition pressure-temperature curve.

As the ABQT significantly affects the elastic properties of quartz (Carpenter et al., 1998), it may be detectable in quartz-rich felsic rocks in the upper crust by seismic methods, as has been demonstrated in laboratory experiments (Kern, 1982). However, these experiments also detected that the elastic properties of the rocks were significantly influenced by the nonhydrostatic stresses and microcracks that originated in the rock samples during rapid heating. Therefore, these experimental results cannot be used directly for precisely characterizing the elastic properties of felsic rocks crossing the ABQT in the deep crust. To do this characterization as precisely as possible, a Landau-type parameterization of the phase transition (Carpenter et al., 1998) was employed to model the elastic properties of pure quartz. Subsequently, the elastic properties of an average granite (Le Maitre, 1976) containing 32 vol% of quartz were calculated by using a known modeling technique and the elastic properties of minerals (Sobolev and Babeyko, 1994). In this modeled granite and for a geotherm with a temperature (T) gradient of 35 °C/km, the ABQT occurs at a depth of 19 km at $T = 700$ °C (Fig. 1A). Reflectivity synthetic seismograms (Fuchs and Müller, 1971) were calculated for an average one-dimensional velocity model for central Tibet incorporating the ABQT at 19 km depth (Fig. 1B). These synthetic seismograms show that the P-wave wide-angle reflection from the ABQT is the dominant phase from 90 to 170 km epicentral distance. In contrast, there is no visible S-wave reflection from the ABQT (Fig. DR1¹). The seismograms also show that the low-velocity zone for P-waves just above the ABQT is insufficient to create a shadow zone in the first arrivals and thus cannot be detected by refraction or wide-angle reflection measurements (Fig. 1B). In summary, the ABQT generates a measurable seismic signature if temperatures of 700 °C or greater are achieved in quartz-rich felsic rocks. The expected seismic features of the ABQT are a 0.3–0.5 km/s increase in P-wave velocity over a depth of ~600 m and a minor change in S-wave velocity. These features have been encountered in the seismic model from the International Deep Profiling of Tibet and the Himalaya (INDEPTH) III profile from central Tibet, where the crust is known to be hot (several independent observations; Alsdorf and Nelson, 1999; Hacker et al., 2000; Wei et al., 2001). Here the seismic model is combined with

*E-mail: Mechie—jimmy@gfz-potsdam.de. Current addresses: Jones—Dublin Institute for Advanced Studies, 5 Merrion Square, Dublin 2, Ireland. Solon—ExxonMobil Exploration Company, Houston, Texas 77060, USA.

†Bock: Deceased 6 November 2002. Nelson: Deceased 17 August 2002.

¹GSA Data Repository item 2004096, Appendix DR1 and Figures DR1–DR3, is available online at www.geosociety.org/pubs/ft2004.htm, or on request from editing@geosociety.org or Documents Secretary, GSA, P.O. Box 9140, Boulder, CO 80301-9140, USA.

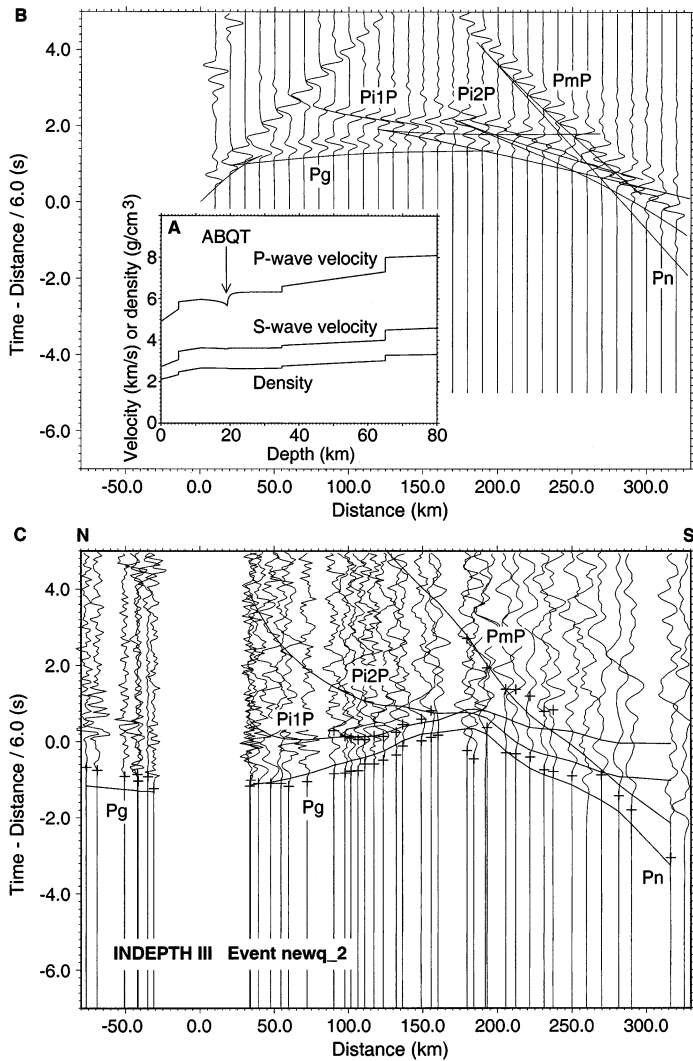


Figure 1. A: P- and S-wave velocities and density vs. depth profiles across α - β quartz transition (ABQT) in typical granite between 11 and 26 km depth, for geotherm with temperature gradient of 35 °C/km. Above 11 km depth and below 26 km depth, average one-dimensional P- and S-wave velocities vs. depth profiles have been derived from two-dimensional P-wave velocity (V_p) model (Zhao et al., 2001) and two-dimensional S-wave velocity model (Fig. 3B). INDEPTH III data require positive vertical velocity gradient for both P- and S-waves down to ~10 km depth. This positive gradient is probably due to closing of cracks and decrease in fluid content with depth which, above ~10 km depth, overrides negative velocity gradient caused by high temperature gradient. Above 11 km depth and below 26 km depth, density (ρ) has been calculated according to $\rho = 0.3788V_p + 0.252$ (Birch, 1961). B: Synthetic seismograms for model shown in Figure 1A. Record section reduced with velocity of 6 km/s shows vertical component of P-wave motion in which each trace is normalized individually. Seismograms have been calculated for dominant frequency of 2 Hz, which is approximately dominant frequency in wide-angle earthquake data shown in C. Continuous lines represent phases calculated from model in Figure 1A. Key: Pg—first-arrival refraction through upper crust; Pi1P—reflection from ABQT (top of middle crust); Pi2P—reflection from top of lower crust; PmP—reflection from Moho; Pn—first-arrival refraction through uppermost mantle. C: Seismic data from event “newq_2,” one of four events at 88.5°E, 33.15°N (Fig. 2), recorded on INDEPTH III array. Record section reduced with velocity of 6 km/s shows vertical component of P-wave motion in which each trace is normalized individually. Continuous lines represent phases calculated from two-dimensional P-wave velocity model (Fig. 4) (Zhao et al., 2001); crosses represent traveltime picks. Although off-line stations are also displayed, only in-line station picks are shown.

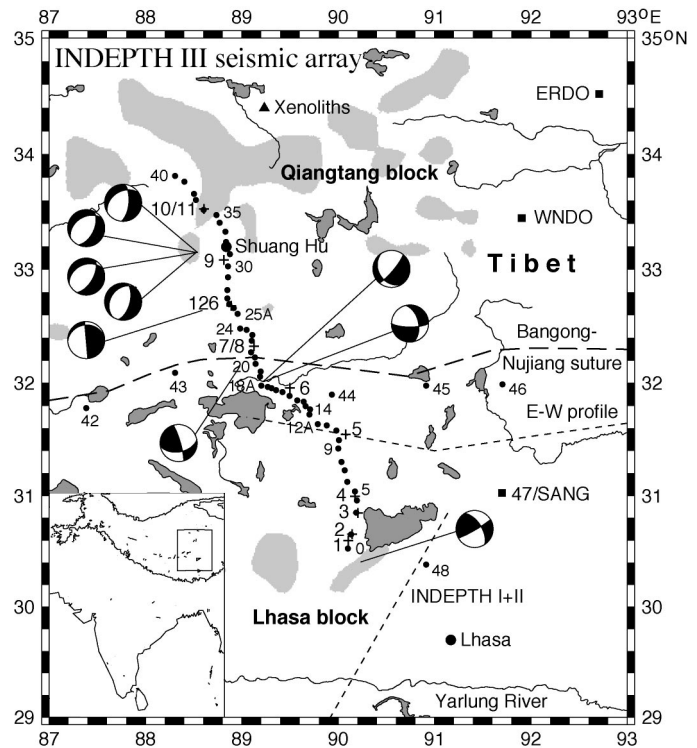


Figure 2. Location map (box within inset) for INDEPTH III array in central Tibet. Crosses and larger numbers represent shots, whereas dots and smaller numbers represent recording stations. Epicentral locations and focal mechanisms of nine earthquakes used to derive two-dimensional S-wave velocity structure beneath INDEPTH III profile are also shown. Locations of INDEPTH I + II traverse (Nelson et al., 1996), previous east-west wide-angle seismic profile (Sapin et al., 1985), and three broadband stations (SANG, WNDO, ERDO) for which crustal structure has been obtained (Owens and Zandt, 1997) are also shown, as is location where xenoliths were found (Hacker et al., 2000). Entire INDEPTH III seismic array is above 4500 m. Ground above 5500 m is shaded light gray; lakes are shaded dark gray. In inset, outline of Tibet plateau, as defined by 3000 m contour, is shown.

magnetotelluric and structural geologic observations to provide an internally consistent interpretation of crustal structure beneath the profile.

INDEPTH III DATA AND INTERPRETATION

Between 1998 and 1999, project INDEPTH carried out a series of active- and passive-source seismic experiments in central Tibet (Fig. 2) during phase III. As part of the active-source experiments, 12 shots along a north-northwest–south-southeast profile, ~400 km long, crossing the Bangong-Nujiang suture at ~89.5°E, were recorded by almost 60 three-component broadband and short-period stand-alone seismographs, mainly at a spacing of 5–10 km. From these wide-angle reflection and refraction measurements, a two-dimensional P-wave velocity model was derived for the whole crust beneath the INDEPTH III profile (Zhao et al., 2001). Although the 12 shots along the profile provided good-quality P-wave data, they provided rather poor quality S-wave data. To address this deficiency, nine earthquakes, located close enough to the profile that they could be used to derive a two-dimensional S-wave velocity model below the profile, were exploited. Details of how the earthquakes were included in the modeling and of the inversion for the two-dimensional S-wave velocity structure are available (Appendix DR1; see footnote 1).

In the P-wave record section shown as an example of one of the earthquakes (Fig. 1C), the reflected phase, Pi1P, is the dominant picked phase between 90 and 140 km epicentral distance. Thus, both in the

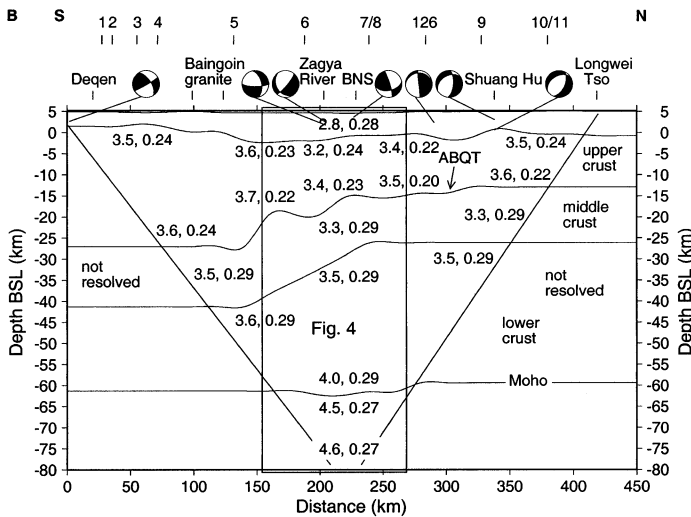
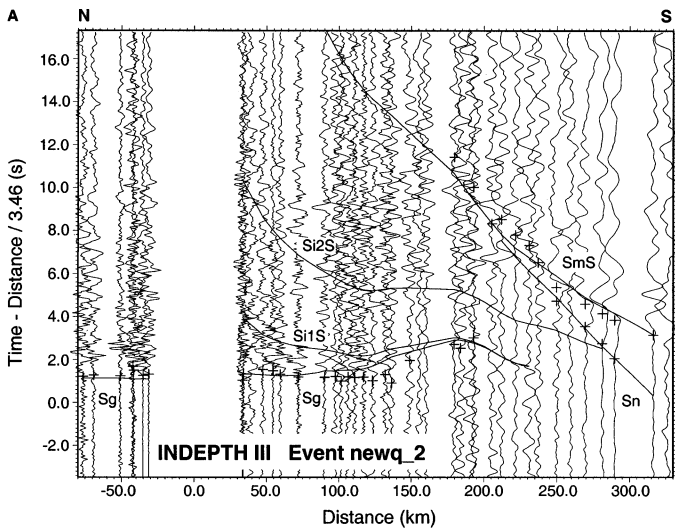


Figure 3. A: Seismic data from event “newq_2,” one of four events at 88.5°E, 33.15°N in Figure 2, recorded on INDEPTH III array. Record section reduced with velocity of 3.46 km/s shows north-south horizontal (approximately radial) component of S-wave motion in which each trace is normalized individually. Continuous lines represent phases calculated from model in B; crosses represent traveltimes. Although off-line stations are also displayed, only in-line station picks are shown. Although there are no observed arrivals for intracrustal reflections Si1S and Si2S, their theoretical positions are shown. Key: Sg—refraction through upper crust; Si1S—reflection from top of middle crust; Si2S—reflection from top of lower crust; SmS—reflection from Moho, Sn—refraction through uppermost mantle. **B:** S-wave velocity and Poisson’s ratio model for INDEPTH III profile in central Tibet. Velocities are in km/s. Focal mechanisms are shown in map-view projections. Locations of shots (see also Fig. 2) used to derive P-wave model (Fig. 4) (Zhao et al., 2001) are shown above model. Box shows that part of model shown together with P-wave velocities and resistivities in Figure 4. ABQT— α - β quartz transition, BNS—Bangong-Nujiang suture; BSL—below sea level.

observed and synthetic record sections, Pi1P is the dominant phase between 90 and 140 km epicentral distance. Beyond 140 km epicentral distance in the observed data, Pi1P interferes with Pi2P, and thus it is impossible to decide which is the dominant phase, whereas in the synthetic data, Pi1P from the ABQT is the dominant phase out to 170 km epicentral distance. At epicentral distances beyond 120 km in the observed data, the Pi1P phase has a somewhat lower apparent velocity, 5.7 km/s, than the value of 5.95 km/s for the reflection from the ABQT in the synthetic data. This discrepancy is due to two-dimensional ve-

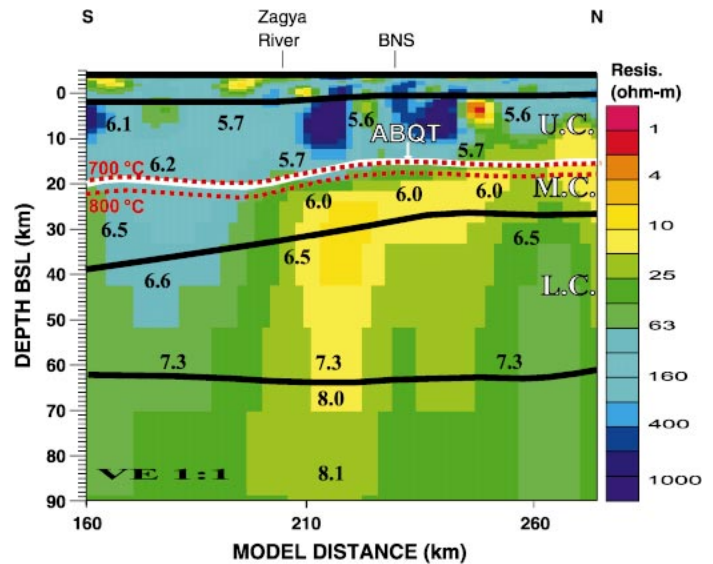


Figure 4. Resistivity model derived by using magnetotelluric data for central part of INDEPTH III profile in vicinity of Bangong-Nujiang suture (BNS) in central Tibet. Resistivity (Resis.) model is overlain by layer boundaries and point P-wave velocities taken from two-dimensional seismic model (Zhao et al., 2001). Hot colors (red and yellow) indicate areas of high conductivity, whereas cold colors (blue and purple) indicate zones of low conductivity. Velocities are in km/s. ABQT— α - β quartz transition, U.C.—upper crust, M.C.—middle crust, L.C.—lower crust; BSL—below sea level. Modified after Solon (2000).

locity variations along the profile. The Pi1P phase can also be observed well in most of the P-wave record sections from the 12 shots (Fig. DR2; see footnote 1) (Zhao et al., 2001). In contrast, in the S-wave record section from the same earthquake (Fig. 3A), arrivals for the reflected phase, Si1S, corresponding to the Pi1P reflection cannot be observed. This fact is also true for the S-wave record sections from the other eight earthquakes.

The average Poisson’s ratio in the top layer of the final model is 0.28 (Fig. 3B). The main upper-crustal layer (second top layer in Fig. 3B) has P-wave velocities of 5.6–6.2 km/s (Zhao et al., 2001) and Poisson’s ratios of 0.20–0.24, indicative of felsic rocks rich in quartz in the α state (Sobolev and Babeyko, 1994; Christensen, 1996). Results from a previous east-west wide-angle seismic profile in the area (Fig. 2) also showed evidence for low Poisson’s ratios in the upper crust (Min and Wu, 1987). For the middle and lower crust (Fig. 3B), the inversion resulted in an average Poisson’s ratio of 0.29. Within the region of resolution, from ~150 km south of the Bangong-Nujiang suture to ~80 km north of the suture, the middle crust has S-wave velocities of 3.3–3.5 km/s, whereas the lower crust has S-wave velocities of 3.5–3.6 km/s at the top, increasing to ~4.0 km/s at the base of the crust.

DISCUSSION AND CONCLUSIONS

The middle and lower crustal layers of the seismic model correlate well with a region of plateau-wide high electrical conductivity in the INDEPTH magnetotelluric (MT) models (Wei et al., 2001). Specifically, for the region of the Bangong-Nujiang suture, detailed modeling has demonstrated that low seismic velocities in the mid-crustal layer correlate with high mid-crustal electrical conductivities that climb closer to the surface than immediately to the south (Fig. 4) (Solon, 2000). In order to explain the high conductivity values beneath the plateau, a combination of aqueous fluids and partial melts has been invoked (Chen et al., 1996; Wei et al., 2001; Li et al., 2003).

From the seismic and MT models and the signature of the ABQT

in a typical felsic rock, it is contended that the boundary between the upper and middle crust beneath the INDEPTH III profile represents the ABQT (white solid line in Fig. 4). This contention is supported by the following facts: (1) It has been argued that the main upper-crustal layer is rich in quartz. (2) In both the theoretical and observed P-wave data, the intracrustal reflection, P11P, is the dominant correlated phase in the record section between 90 and 140 km epicentral distance. (3) Downward across the boundary, a P-wave velocity increase of 0.2–0.4 km/s (Fig. 4) is accompanied by only a minor change in S-wave velocity (Fig. 3B), which is also expected for the ABQT. (4) A few kilometers below the boundary, temperatures high enough to cause partial melting of quartz-rich felsic rocks can be expected and are interpreted, in keeping with the combination of aqueous fluids and partial melts being the cause of the high conductivities observed in the middle crust beneath the profile. (5) Geologic maps and tectonic models (Appendix DR1 and Fig. DR3; see footnote 1) indicate that the INDEPTH III region of central Tibet is underlain by quartz-rich upper and middle crust and that the ABQT does not likely coincide with a major lithologic or structural boundary within the Tibetan crust.

The boundary between the upper and middle crust, representing the ABQT, is at 32 ± 3 km depth (pressure = 850 ± 85 MPa; average density of upper crust = 2700 kg/m^3), ~ 150 km south of the Bangong-Nujiang suture (Zhao et al., 2001). Thus a temperature of $770\text{--}815$ °C at this depth and an average temperature gradient of 25 °C/km are suggested ~ 150 km south of the suture. North of the suture, this boundary rises to 18 ± 2 km (480 ± 50 MPa), which corresponds to $685\text{--}710$ °C at this depth and an average temperature gradient of 39 °C/km. Very high temperature in the upper crust north of the suture is consistent with the high electrical conductivity anomaly just below the ABQT (Fig. 4). This anomaly most likely reflects a high degree of partial melting of the biotite-bearing felsic rocks at $800\text{--}900$ °C, which is the temperature that must be achieved 3–5 km below the ABQT boundary. Unusually high temperatures in the crust north of the suture are also consistent with low seismic velocities in the upper and middle crust (Figs. 3B and 4), seismicity being confined to the upper crust (Langin et al., 2003), absence of the Sn seismic phase (Ni and Barazangi, 1983; McNamara et al., 1995), and temperature estimates from crustal xenoliths (Hacker et al., 2000). It is interesting to note that the high conductivities and presumably high degrees of partial melting just below the ABQT are absent south of the Bangong-Nujiang suture in the northern Lhasa block (Fig. 4). Farther south in the Yadong-Gulu rift in the southern Lhasa block, where the INDEPTH I + II traverse is located (Fig. 2), there is evidence for high degrees of partial melting in the middle crust (Nelson et al., 1996). This fact may indicate a strong variability of water content in the middle crust of Tibet. In view of the results of this study, the petrologic interpretation of similar mid-crustal seismic boundaries in other areas of thick, hot crust should be reexamined. Although it cannot be wholly excluded that the boundary between the upper and middle crust beneath the INDEPTH III profile is due to other causes, e.g., lithologic changes, in regions with thick, hot, quartz-rich felsic crust (e.g., Tibet or the Altiplano), the ABQT must be crossed and, as has been shown here, provides a complete explanation of the seismic observations in terms of recent geological processes rather than lithologic changes.

ACKNOWLEDGMENTS

We thank the Ministry of Land and Resources of China, the National Natural Science Foundation of China, the U.S. National Science Foundation, the Deutsche Forschungsgemeinschaft, and the GeoForschungsZentrum Potsdam (GFZ) for financial support during the project. We are also grateful to the personnel of the 5th Geophysical Exploration company of the Ministry of Land and Resources for their logistical support and for drilling and executing the shots of the controlled-source survey. The instruments were provided by IRIS-PASSCAL and the GFZ Potsdam geophysical instrument pool.

REFERENCES CITED

- Alsdorf, D., and Nelson, D., 1999, Tibetan satellite magnetic low: Evidence for widespread melt in the Tibetan crust?: *Geology*, v. 27, p. 943–946.
- Birch, F., 1961, The velocity of compressional waves in rocks to 10 kilobars, part 2: *Journal of Geophysical Research*, v. 66, p. 2199–2224.
- Carpenter, M.A., Salje, E.K.H., Graeme-Barber, A., Wruck, B., Dove, M.T., and Knight, K.S., 1998, Calibration of excess thermodynamic properties and elastic constant variations associated with the α - β phase transition in quartz: *American Mineralogist*, v. 83, p. 2–22.
- Chen, L., Booker, J.R., Jones, A.G., Wu, N., Unsworth, M.J., Wei, W., and Tan, H., 1996, Electrically conductive crust in southern Tibet from INDEPTH magnetotelluric surveying: *Science*, v. 274, p. 1694–1696.
- Christensen, N.I., 1996, Poisson's ratio and crustal seismology: *Journal of Geophysical Research*, v. 101, p. 3139–3156.
- Fuchs, K., and Müller, G., 1971, Computation of synthetic seismograms with the reflectivity method and comparison with observations: *Royal Astronomical Society Geophysical Journal*, v. 23, p. 417–433.
- Hacker, B.R., Gnos, E., Ratschbacher, L., Grove, M., McWilliams, M., Sobolev, S.V., Wan, J., and Zhenhan, W., 2000, Hot and dry deep crustal xenoliths from Tibet: *Science*, v. 287, p. 2463–2466.
- Jaoul, O., Tullis, J., and Kronenberg, A., 1984, The effect of varying water contents on the creep behaviour of Heavite quartzite: *Journal of Geophysical Research*, v. 89, p. 4298–4312.
- Kern, H., 1982, Elastic-wave velocity in crustal and mantle rocks at high pressure and temperature: The role of the high-low quartz transition and of dehydration reactions: *Physics of the Earth and Planetary Interiors*, v. 29, p. 12–23.
- Langin, W.R., Brown, L.D., and Sandvol, E.A., 2003, Seismicity of central Tibet from project INDEPTH III seismic recordings: *Seismological Society of America Bulletin*, ser. A, v. 93, p. 2146–2159.
- LeChatelier, H., 1889, Sur la dilatation du quartz: *Paris Académie des Sciences Comptes Rendus*, v. 108, p. 1046.
- Le Maitre, R.W., 1976, The chemical variability of some common igneous rocks: *Journal of Petrology*, v. 17, p. 589–637.
- Li, S., Unsworth, M.J., Booker, J.R., Wei, W., Tan, H., and Jones, A.G., 2003, Partial melt or aqueous fluid in the mid-crust of southern Tibet? Constraints from INDEPTH magnetotelluric data: *Geophysical Journal International*, v. 153, p. 289–304.
- McNamara, D.E., Owens, T.J., and Walter, W.R., 1995, Observations of regional phase propagation across the Tibetan Plateau: *Journal of Geophysical Research*, v. 100, p. 22,215–22,229.
- Min, Z., and Wu, F.T., 1987, Nature of the upper crust beneath central Tibet: *Earth and Planetary Science Letters*, v. 84, p. 204–210.
- Nelson, K. D., and 27 others, 1996, Partially molten middle crust beneath southern Tibet: Synthesis of project INDEPTH results: *Science*, v. 274, p. 1684–1688.
- Ni, J., and Barazangi, M., 1983, High-frequency seismic wave propagation beneath the Indian Shield, Himalayan arc, Tibetan Plateau and surrounding regions: High uppermost mantle velocities and efficient Sn propagation beneath Tibet: *Royal Astronomical Society Geophysical Journal*, v. 72, p. 665–689.
- Owens, T.J., and Zandt, G., 1997, Implications of crustal property variations for models of Tibetan Plateau evolution: *Nature*, v. 387, p. 37–43.
- Sapin, M., Wang, X.-J., Hirn, A., and Xu, Z.X., 1985, A seismic sounding in the crust of the Lhasa block, Tibet: *Annales Geophysicae*, v. 3, p. 637–646.
- Sobolev, S.V., and Babeyko, A.Y., 1994, Modelling of mineralogical composition, density and elastic wave velocities in the unhydrated rocks: *Surveys in Geophysics*, v. 15, p. 515–544.
- Solon, K.D., 2000, Electromagnetic images of the Bangong-Nujiang suture zone of central Tibet: From INDEPTH-III magnetotelluric data [M.S. thesis]: Syracuse, New York, Syracuse University, 81 p.
- Wei, W., Unsworth, M., Jones, A., Booker, J., Tan, H., Nelson, D., Chen, L., Li, S., Solon, K., Bedrosian, P., Jin, S., Deng, M., Ledo, J., Kay, D., and Roberts, B., 2001, Detection of widespread fluids in the Tibetan crust by magnetotelluric studies: *Science*, v. 292, p. 716–718.
- Zhao, W., Mechie, J., Brown, L.D., Guo, J., Haines, S., Hearn, T., Klemperer, S.L., Ma, Y.S., Meissner, R., Nelson, K.D., Ni, J.F., Pananont, P., Rapine, R., Ross, A., and Saul, J., 2001, Crustal structure of central Tibet as derived from project INDEPTH wide-angle seismic data: *Geophysical Journal International*, v. 145, p. 486–498.

Manuscript received 2 December 2003

Revised manuscript received 29 March 2004

Manuscript accepted 1 April 2004

Printed in USA